Chapter 11
Laser-Induced Engineering of Surface Structures and Properties on Oxygen-Adsorbed TiC(111) Surface: First-Principles Calculations

V. V. Ilyasov, B. C. Meshi, D. K. Pham, Ch. V. Nguyen, O. M. Holodova, T. P. Zhdanova, I. V. Ershov, N. V. Prutsakova and I. G. Popova

Abstract In this chapter, we used the density functional theory (DFT) to systematically investigate the electron structure and elastic moduli of oxygen-adsorbed O/Ti_xC_y(111) surface affecting its potential reconstructions with laser. For the first time we studied within the density functional theory framework the local atomic and electron structures of potential O/Ti_xC_y(111) surface configurations as well as their thermodynamic and elastic properties. A considerable rearrangement has been established in the local atomic structure of O/TiC(111) surface depending upon the degree of its coverage with atomic oxygen in FCC stacking position. We have demonstrated that the distance between adsorbate and TiC(111) surface decreased with the increase of its coverage with oxygen. Additionally, the effect of oxygen adsorbed on the Ti_xC_y(111) surface on the electronic properties in its different reconstructions has been also studied. The results showed that a correlation between the energy level of flat bands in the −5.1 eV and −5.7 eV energy regions was responsible for the doublet of singular peaks corresponding to partial densities of oxygen 2*p* electrons, and the bond energy and adsorption energy of oxygen atom in non-stoichiometric O/TiC_y(111) systems. Effective charges of titanium and carbon atoms surrounding the oxygen adatom in various reconstructions have been identified. We have established charge transfer from titanium atom to oxygen and carbon atom,s determined by the reconstruction of local atomic and electron structures and correlating with their electronegativity values and chemisorption processes. Calculated values of elastic moduli for the upper part of ultrathin O/TiC

V. V. Ilyasov (✉) · B. C. Meshi · D. K. Pham · O. M. Holodova · T. P. Zhdanova
I. V. Ershov · N. V. Prutsakova · I. G. Popova
Don State Technical University, Rostov-on-Don, Russia
e-mail: viily@mail.ru

Ch.V. Nguyen
School of Mechanical Engineering, Le Quy Don Technical University, Hanoi, Vietnam

I. A. Parinov et al. (eds.), *Advanced Materials*, Springer Proceedings in Physics 207, https://doi.org/10.1007/978-3-319-78919-4_11

(111) and O/Ti_xC_y(111) layers correlate well with experimental findings and other theoretical results. Potential mechanisms for laser nanostructuring of titanium carbide surface have been suggested.

11.1 Introduction

Surface properties of ultrathin titanium carbide (TiC) films remain in the focus of attention owing to their extraordinary physical properties, such as high thermal and electric conductivity, high hardness, durability [1–3]. Stoichiometric TiC has plain B1 crystal structure. However, TiC films typically contain vacancies both in the titanium sublattice and carbon sublattice [4]. In order to understand the physical properties of such materials, it is necessary to investigate the atomic behavior of the TiC crystals [5]. There are many ways to modulate the surface properties of TiC materials, one of the most used methods is the laser surface nanostructuring [6], which includes melting, cooling, and crystallization [7, 8]. In order to adjust these methods exactly, we can modulate the energy density and laser pulse duration. Recently, numerical experimental and theoretical investigations on the structural properties of the TiC(111) surface showed that the TiC(111) surface with Ti-terminated is the polar surface [9–11].

Currently, from He^+ ion scattering spectroscopy, Souda et al. [12] showed that when an oxygen was adsorbed on the TiC(111) surface, the (1×1) and $(\sqrt{3} \times \sqrt{3})$ *R*30 types of atomic structures were formed. Additionally, it was shown that at room temperature the TiC(111)-(1 × 1)-O structure is stable [13], whereas it reconstructed to TiC(111)-$(\sqrt{3} \times \sqrt{3})$ *R*30-O form, when the temperature heated up to 1000 °C [13, 14]. The results also indicated that the positions in the face-centered cubic (FCC) arrangement can be occupied by adsorbed oxygen atoms [14].

As above-mentioned, reconstructions of TiC(111) atomic surface are manifested in the electron spectrum of titanium and carbon subsystems, and also in the elastic constants and moduli of the top layer similarly to the O/TiC(001) system [15]. Recently, Marques et al. [4] by using a three-dimensional (3D) model of bulk TiC crystal have studied the effect of an oxygen atom on the structural, electronic and mechanical properties of TiC_xO_y structure. They indicated that the lattice parameters and elastic constants of the TiC_xO_y system decrease with increasing oxygen content. Edamoto et al. have studied the electronic state of oxygen adsorbed on a TiC surface by using angle-resolved photoemission electron microscopy [13]. In comparison with the $2p_z$ orbital, it was shown that for chemisorption processes the $2p_{x,y}$ orbitals of oxygen atom are the most essential for the TiC surface. The atomic, electronic and thermodynamic properties of adsorption of atoms in the three first periods on the TiC(111) surface have been also investigated from first principles calculations [11]. By using DFT method, Wang et al. also investigated the structural and electronic properties of TiC(110) surface [5].

Up-to-date, the electronic and elastic properties of oxygen-adsorbed TiC(111) surface with distributed Ti and C vacancies has not yet been studied thoroughly. Thus, in this work we focus on the electronic and elastic properties of the O/Ti_xC_y(111) system upon thermal action using DFT method from first principles calculations.

11.2 Model and Method

Theoretical study of the O/TiC(111) system is based on three-dimensional periodic slab model. Titanium-terminated supercell consisting of 2 × 2 unit cells arranged within a plane (111) was used. Figure 11.1a demonstrates a fragment of the TiC (111) slab, in Fig. 11.1b potential positions of the oxygen atom are shown. We have studied 6 various configurations of oxygen atom positions on a TiC(111) slab: A—Oxygen atom situated above the Ti atom of the top layer; B—Oxygen atom situated above the Ti atom of the third layer (FCC hollow); C—Oxygen atom situated on carbon atom of second layer (HCP hollow); D—Oxygen atom situated in the bridge site; A_{vak}—Oxygen atom situated above the surface vacancy of the Ti atom in top layer; C_{vak}—Oxygen atom situated above the vacancy of the carbon atom in second layer.

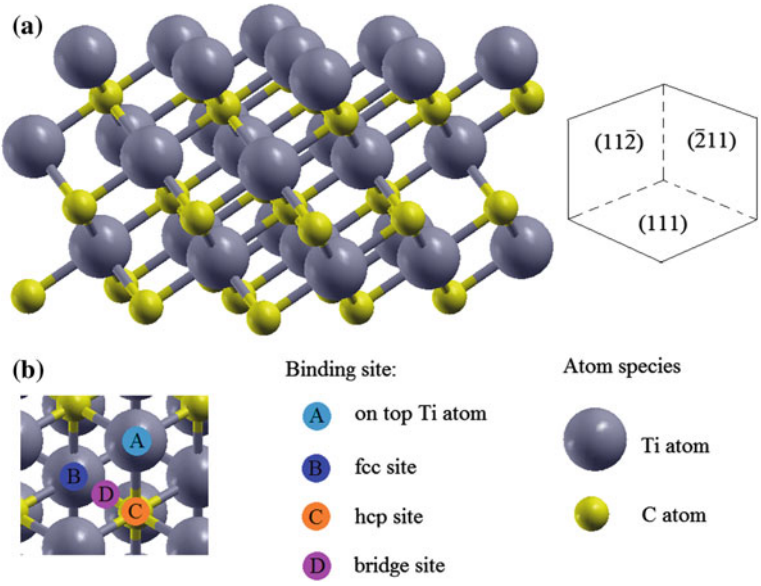

Fig. 11.1 TiC(111) surface model (**a**) and binding positions of oxygen atom (**b**) on TiC(111) surface, top view

FCC hollow position (in our case, B) is known [11] to be a relatively stable binding site for O atom on TiC(111) surface. Therefore, we have performed calculations for oxygen in B position for the coverage range from 1/9 to a complete monolayer. All coverage values of $\Theta = 0.11, 0.22, 0.33, 0.44, 0.55$ and 1.0 were calculated based on the (111) plane of a (2×2) TiC supercell. In particular, $\Theta = 0.33$ coverage corresponds to the TiC(111)-$(\sqrt{3} \times \sqrt{3})$ $R30$-O reconstruction, while the coverage $\Theta = 1.0$ corresponds to the TiC(111)-(1×1)-O structure.

TiC(111) slab represents six non-equivalent alternating Ti and C layers in the [111] direction. Vacuum gap of 12 Å excluded any interactions between the slab translations in the [111] direction. In this study self-consistent calculations were carried, based on the density functional theory (DFT) within pseudopotential method (Quantum Espresso code) [16]. Exchange and correlation were taken into account using PBEsol functionals (GGA approximation) [17, 18]. The plane waves expansion cutoff energy of 400 eV was used. The convergence test for the surface energy and interplanar distance confirmed the cutoff energy of 400 eV and a $3 \times 3 \times 1$ Monkhorst-Pack grid were sufficient [19]. The SCF unit cell total energy convergence was at least 10^{-6} Ry/cell. To describe the interaction between valence electrons and the core, Vanderbilt ultrasoft pseudopotentials were used. The pseudopotentials were generated using Troullier-Martins scheme [20]. The following electronic configurations were used: Ti—[Ar]$3d^2 4\ s^2$, O—[He]$2s^2 2p^4$, C—[He]$2s^2 2p^2$. [Ar] and [Ne] were considered as core states.

The effective charges were estimated on the oxygen atom as well as on the surface Ti and C nearest atoms in six O-adsorbed O/Ti_xC_y(111) models using Löwdin population analysis [21].

Elastic properties of the O/Ti_xC_y(111) and O/TiC(111) systems were theoretically studied using Elastic program [22], based on DFT total energy calculations for deformed crystal structures. Elastic constants $c_{i,j}$ determine the crystal response to applied external forces and characterize the bulk modulus B, as well as Young's modulus E, shear modulus G, and Poisson's ratio υ [23]. Cubic systems are usually represented by 3 independent elastic constants c_{11}, c_{12}, and c_{44} [3]. Elastic constants were calculated using the stress-strain approximation, based on generalized Hooke's law. The Voigt-Reuss-Hill (VRH) approximation was used to estimate bulk modulus B, shear modulus G, and Young's modulus E. The approximation provides the best estimation of mechanical properties of polycrystalline materials based on elastic constants and the formulas in [22, 23].

11.3 Results and Discussion

11.3.1 Energy and Atomic Structure of Oxygen-Adsorbed $Ti_xC_y(111)$ Surfaces

To study the electron structure and elastic moduli of O-adsorbed O/Ti_xC_y(111) surface, relaxation of two upper atomic layers (Ti, C) of a TiC slab with adsorbate was made. Initially, the O atom was placed in the binding sites (Fig. 11.1) at the distance of 2 Å from the TiC(111) surface. Two lower atomic layers of the 2D O/Ti_xC_y(111) system considered "frozen". Relaxation was carried out until the total force in the system reduced to 0.001 eV/Å. Atomic structures of a three-layer slab with oxygen in various configurations of the O/Ti_xC_y(111) and O/TiC(111) systems after relaxation are shown in Fig. 11.2. Table 11.1 offers the calculated parameters of atomic structures, including the lengths of bonds d_{Ti-O} and d_{Ti-C} between the oxygen atom and its nearest neighbors, vertical distances: d_0—between the adsorbate and the first Ti layer, d_1—between the first Ti layer and C layer, d_2—between the C layer and the third Ti layer, total energy of the substrate with oxygen E_{tot}, total energy of the original substrate surface E_{ref} for oxygen binding sites on the surface of TiC(111) and Ti_xC_y(111) slabs. It also contains some known theoretical and experimental findings correlating with the data of this DFT calculation.

Analysis of Table 11.1 shows that the processes of oxygen chemisorption result in considerable rearrangement of the local atomic structure of O/Ti_xC(111) and O/TiC_y(111) surfaces in comparison with O/TiC(111). For the FCC hollow binding site, we have performed calculations of coverage with atomic oxygen ranging from 1/9 to a complete monolayer. Table 11.2 offers calculated parameters of atomic structures for all coverage values of $\Theta = 0.11, 0.22, 0.33, 0.44, 0.55$, and 1.0, including vertical distances d_0, d_1, and d_2, pointed in Table 11.1, adsorption energy E_{ads}, the effective charge on the oxygen atom and the nearest Ti and C atoms. It also contains some known findings correlating with the data of these DFT calculations.

Analysis of Table 11.2 allows one to observe a considerable rearrangement in the local atomic structure of O/TiC(111) surface depending upon the degree of its coverage with atomic oxygen. In particular, the distance between adsorbate and (111) surface decreases with the increase of its coverage with oxygen. Atomic structure reconstruction may be caused by charge transfer from Ti atoms to C atoms, resulting in stronger electrostatic interaction between Ti and C atoms. Changes in the d_1 and d_2 distances in various atomic configurations of the O/TiC (111) surface depending on its coverage with oxygen are of specific interest. Calculation results in Table 11.2 demonstrate that the increase of oxygen coverage is followed by an increase of the distance between the layers of Ti and C atoms in the surface layers to d_1 = 1.314 Å with a simultaneous decrease of the distance d_2 = 1.244 Å (at $\Theta = 1.0$).

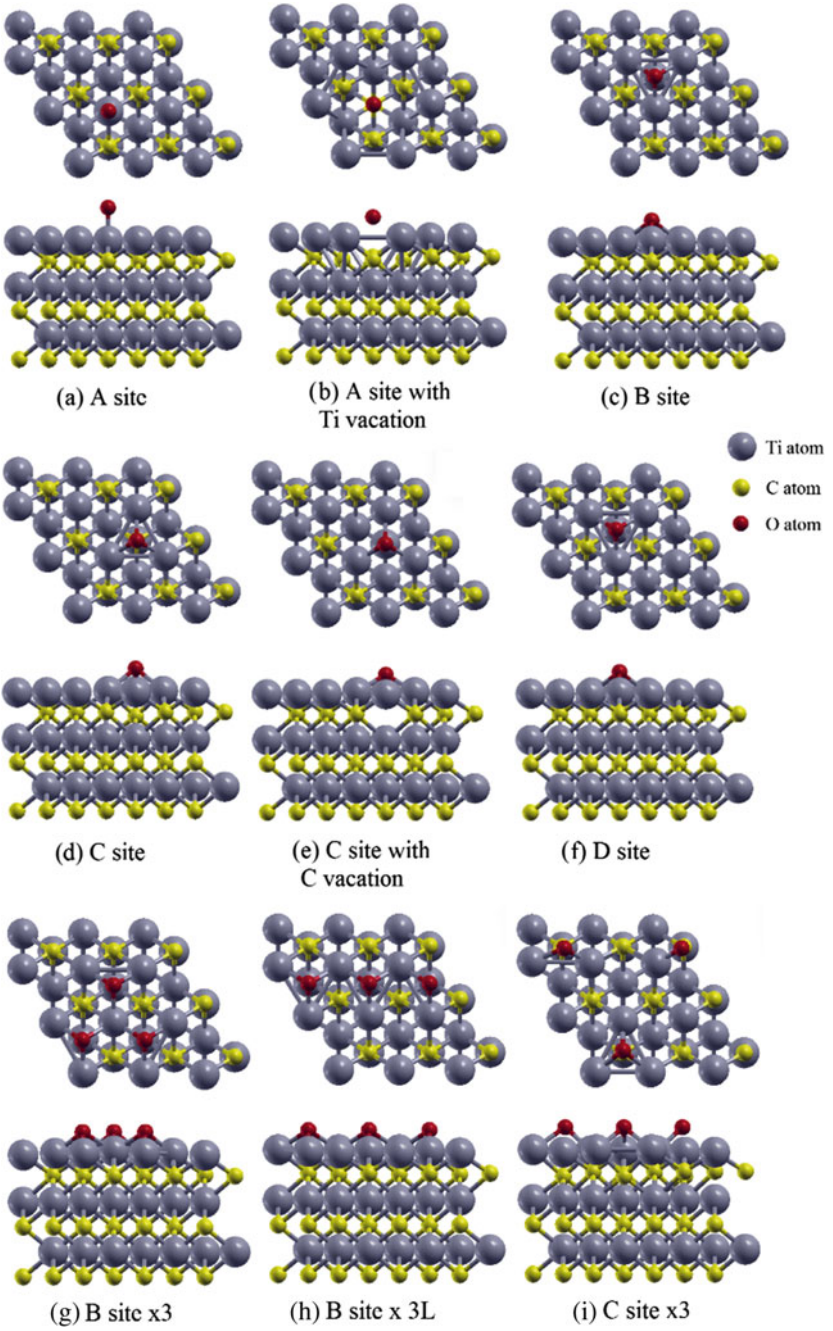

Fig. 11.2 Supercells of the atomic structure surface (**a**, **c**, **d**, **f**) in the O/TiC(111) system, **b**, **e** the O/Ti_xC_y(111) system, and **g–i** the 3-O/TiC(111) system after relaxation (side and top views)

Table 11.1 Bond lengths d_{Ti-O} and d_{Ti-C}, vertical distance d_O between the oxygen atom and TiC (111) surface, distances d_1 and d_2 between layers of Ti and C atoms in three surface layers, total energy E_{tot} of the surface with oxygen, total energy E_{ref} of the original surface

Phase (O-atom position)	d_{Ti-O} (Å)	d_{Ti-C} (Å)	d_O (Å)	d_1 (Å)	d_2 (Å)	E_{tot}	E_{ref}
						Ry	
TiC(111)	–	–	–	1.041 1.010 [11] 0.87 [24]	1.354 1.388 [11]	–	−3456.5663
O/TiC (A)	1.71	2.09	1.709	1.037	1.356	−3488.7557	−3456.5663
O/TiC (B)	1.97	2.06	1.105	1.069	1.349	−3488.9248	−3456.5663
O/TiC (C)	2.01	2.09	1.214	1.065	1.347	−3488.8641	−3456.5663
O/TiC (D)	1.97	2.06	1.105	1.069	1.347	−3488.9249	−3456.5663
O/TiC(A–Ti_{vac})	3.13	1.99	1.057	1.053	1.346	−3371.6716	−3339.7200
O/TiC(C–C_{vac})	1.94	2.12	0.971	1.064	1.344	−3477.3891	−3445.0028

Table 11.2 Distance d_O between oxygen atoms and TiC(111) surface, distances d_1 and d_2 between the layers of Ti and C atoms in three surface layers, adsorption energy E_{ads}, effective charge on the oxygen atom and nearest Ti and C atoms in the B position (FCC site) at various coverage degrees

Degree of oxygen coverage	d_O (Å)	d_1 (Å)	d_2 (Å)	E_{ads} (eV/atom)	Effective charge		
					Ti	C	O
0.11	1.105	1.069	1.349	−10.68	1.05 1.34 [11]	−1.09 −1.68 [11]	−0.78 −1.17 [11]
0.22	1.089	1.097	1.338	−10.60	1.06	−1.11	−0.78
0.33	1.072	1.119	1.329	−10.47	1.07	−1.07	−0.78
0.44	1.055	1.147	1.319	−10.42	1.09	−1.10	−0.77
0.55	1.028	1.172	1.311	−10.34	1.23	−1.12	−0.76
1.0	0.894 0.891 [11]	1.314 1.314 [11]	1.244 1.253 [11]	−9.93 −8.12 [11]	1.42	−1.13	−0.73

We should note that coverage increase from $\Theta = 0.11$ to $\Theta = 1.0$ insignificantly affects the adsorption energy value. The highest adsorption energy was found at the coverage degree of $\Theta = 0.11$ reaching $E_{ads} = -10.68$ eV/atom. In that position the effective charge accumulated by the O atom was −0.78e, titanium atom +1.05e, carbon atoms −1.09e. The adsorption energy at the coverage degree of $\Theta = 1.0$ reached $E_{ads} = -9.93$ eV/atom, which is 1.2 times higher than the data in [11].

11.3.2 Electron Structure of Oxygen-Adsorbed $Ti_xC_y(111)$ Surfaces

The noted rearrangement of local atomic structure significantly affects the electronic energy spectrum of titanium, carbon and oxygen surface atoms in the $O/Ti_xC_y(111)$ systems examined above. Calculation of the band structure of these systems, demonstrated in Fig. 11.3, reveals dependence upon the local atomic structure, and corresponds to the metallic type. Total and partial densities of electron states, also shown in Fig. 11.3, characterize the peculiarities of chemical bond with adsorbed oxygen atom on (111) TiC surface. We should note hybridization occurring between 2*p* orbitals of oxygen and carbon atoms and 3*d* orbitals of titanium atoms. It is indicated by matching of the energy peaks of occupied states in O, C, and Ti atoms (Fig. 11.3).

Several features should be noted in the band spectrum of non-stoichiometric $O/Ti_xC(111)$ configuration in position A shown in Fig. 11.3a. In particular, the hybridization of oxygen 2*p* orbitals with titanium 3*d* orbitals results in the formation of a broad +(1.9–2.3) eV peak of unoccupied electronic states in O/Ti_xC (111). The +0.07 eV peak of the total density of states (Fig. 11.3a) is formed predominantly by unsaturated bonds of oxygen, carbon and titanium surface atoms of the $O/Ti_xC_y(111)$ system. The peak at the Fermi level is mainly formed by contributions from 3*d* states of the surface Ti atoms with a small contribution of 2*p* states of carbon and oxygen atoms. The peak of total DOS is present in all

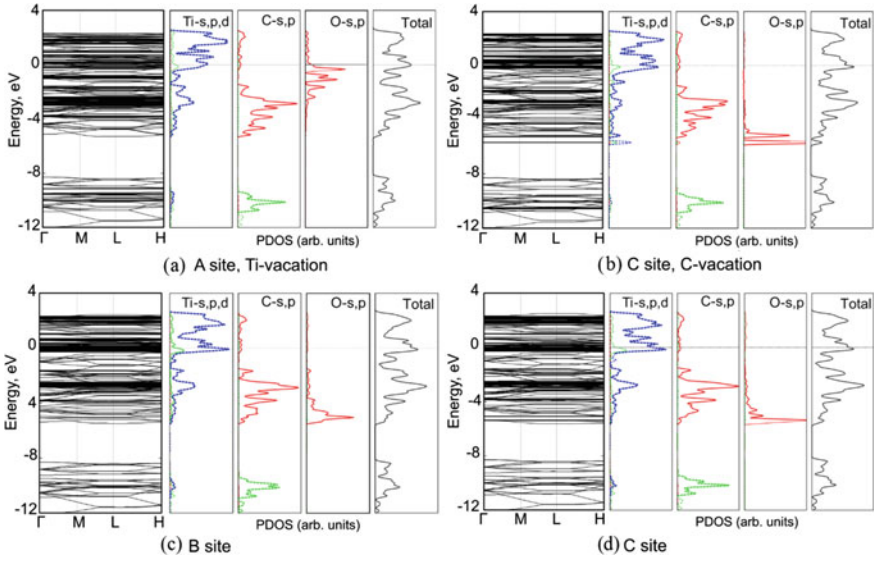

Fig. 11.3 DFT calculation of the band spectrum, partial DOS for Ti, C and O atoms, and total DOS in the binding sites on (111) surface: **a**, **b** O/Ti_xC_y, **c** O/TiC (FCC site), **d** O/TiC (HCP site); partial DOS: s—green, p—red, d—blue, total DOS—black

surface configurations of TiC(111) with and without adsorbate, which have been studied. Bonding states are associated with a strong covalent interaction, characterized by hybridization of Ti_{3d}–C_{2p} atomic orbitals in the −2.5 to −3.8 eV energy interval, and defining the main properties of adsorbing titanium carbide surface. Modification of local atomic structure induced by non-stoichiometry and atomic oxygen adsorption results in a change of the electronic structure. In particular, the electron spectrum is characterized by Ti_{3d}–C_{2p}–O_{2p} hybridization in the energy intervals of 0 to −0.7 eV and −1.5 to −2.3 eV, which is manifested in the band structure and partial DOS in Fig. 11.3a. Statistical weight of partial states should be noted for the electrons participating in hybridization of Ti_{3d}–C_{2p}–O_{2p} orbitals. Analysis of Fig. 11.3a shows that the overlapping regions between 2*p* orbitals of atomic oxygen and Ti_{3d} and C_{2p}-orbitals are insignificant, in agreement with low value of the O atom adsorption energy (−5.14 eV/atom). The latter should be related to the absence of partial states of oxygen in the −2.5 to −3.8 eV energy region, representing the main part of occupied partial states of Ti and C atoms. Comparison of the electronic structure of this atomic configuration with the stoichiometric system O/TiC(111) reveals a different picture. In particular, the overlapping regions between 2*p*-orbitals of atomic oxygen and Ti_{3d} and C_{2p}-orbitals are significant, in agreement with higher value of the O atom adsorption energy in the Ti-top position.

Electronic structure has some new features in case of non-stoichiometric O/TiC_y(111), where O atom takes up the position above the C atom vacancy in the second layer of the slab (Fig. 11.3b). In that configuration bond length amounts d_{O-Ti} = 1.94 Å, which determines a strong chemical bonding between the O atoms and their nearest Ti neighbors. In particular, the energy of chemical bond of O atom on TiC_y(111) surface amounts E_{coh} = 5.7 eV. We refer the estimation of bond energy E_{coh} with the positions of two sharp peaks corresponding to the O_{2p} states in the −5.1 and −5.7 eV interval of energies (Fig. 11.3b). The main part of partial DOS of C and Ti atoms lies in the −1.9 to −3.7 eV interval of energies; it characterize the main properties of the O/TiC_y(111) system. This energy region is represent by a wide band of partial densities of states of Ti and C. The −4.5 to −5.7 eV interval of energies presents mixing between partial states of O, C, and Ti electrons, which plays major role in formation of the corresponding bond and determines the adsorption energy. The maximum value of the adsorption energy of O atom on non-stoichiometric TiC_y(111) surface amounts E_{ads} = −11.06 eV/atom. The increase of the E_{ads} in this configuration correlates with the existence of flat bands (−5.1 and −5.7 eV) in the band structure and is responsible for the double peaks reflecting the O_{2p} electron states.

We should note that a similar correlation was found in stoichiometric O/TiC (111) system with the O atom in B and C positions (Fig. 11.2c, d). In particular, Fig. 11.3c presents two flat bands in the band structure within the −4.6 to −5.0 eV interval of energies responsible for the partial densities of O_{2p} electrons. In the electronic band structure of the atomic configuration (Fig. 11.2c), these flat bands are located almost in the same energy interval as in the previous configuration (Fig. 11.2e). Hence the adsorption energy of atomic oxygen in that configuration is

high (−10.68 eV/atom). The main feature of the stoichiometric O/TiC(111) electronic structure in position C (Fig. 11.2d) is the correlation similar to the one described above. The band spectrum (Fig. 11.3d) of this configuration features three flat bands with the energy of −4.9, −5.1, and −5.3 eV corresponding to sharp peaks of partial densities of O and C_{2p} electrons. These peaks represent hybridization of C_{2p}–O_{2p} orbitals, with partial mixing of Ti_{3d} orbitals. The main part of partial DOS of C and Ti atoms is into −2.1 to −4.9 eV energy interval. This energy interval reveals hybridization between C_{2p}–Ti_{3d} orbitals of C and Ti atoms. The −2.1 to −4.9 eV interval of energies presents a small mixing of partial states of O, C, and Ti electrons, which is caused by adsorption. Average value of the bond energy for O atom in position C is E_{coh} = 5.2 eV, correlating with high adsorption energy (−9.85 eV/atom).

Figure 11.4a–c demonstrate typical peculiarities of the electron structure of a O/TiC(111) system, where three O atoms occupy position B (or C), forming triangular and trimeric clusters on the surface (see Fig. 11.2g–i). In particular, bond length in the triangular configuration is d_{O-Ti} = 1.96 Å; the fact determines a tight chemical bond between the atoms of oxygen and their nearest titanium neighbors. Among other factors, the chemical bond energy of oxygen atom on TiC(111) surface is E_{coh} = 5.2 eV. We associate the estimate of bond energy E_{coh} with the position of main peak reflecting the states of oxygen 2*p* electrons in the −5.2 eV energy region (Fig. 11.4a).

The main part of partial DOS of carbon and titanium atoms is into −1.5 to −3.3 eV interval of energies; it determines the basic properties of the 3-O/TiC(111) system. The energy of −2.8 eV exhibits hybridization between C_{2p}–Ti_{3d} orbitals. Mixing between partial states of O, C, and Ti electrons into −3.5 to 5.4 eV interval of energies plays a decisive role in forming of the corresponding chemical bond and adsorption energy. A comparison was performed between the electron spectrum of total oxygen DOS in triangular configuration with a similar spectrum in the configuration with a single oxygen atom (Fig. 11.3c) in the same binding site. Analysis has shown that the rearrangement in the atomic structure of 3-O/TiC(111) surface noted above is manifested in a change in the electron energy spectrum of the system. In particular, the maximum positions and the shape of peaks for the energies of −1.8, −2.8, and −5.2 eV indicate strengthening of the chemical bond between carbon, titanium, and oxygen atoms. The shift in the energy is $\Delta E = 0.1-0.6$ eV.

In the trimeric configuration (Fig. 11.2h) average length of the bond between oxygen atom and its nine nearest neighbors is d_{O-Ti} = 1.98 Å. The energy of the hybridized ground state of C_{2p}–Ti_{3d} electrons is −2.6 eV, which is 0.2 eV higher than in triangular configuration in the same FCC position. In our opinion, position of the major peak of oxygen 2*p* electrons in the −(4.0–5.0) eV interval of energies shown in Fig. 11.4b determines the character and intensity of chemical bond between the oxygen atoms and TiC(111) film surface. In this configuration, the Ti–O chemical bond is largely ionic, as indicated by the shape of the electron energy spectrum in Fig. 11.4b. In a triangular cluster (Fig. 11.2i), formed by oxygen atoms on TiC(111) surface in HCP positions, the average length of the bond between the

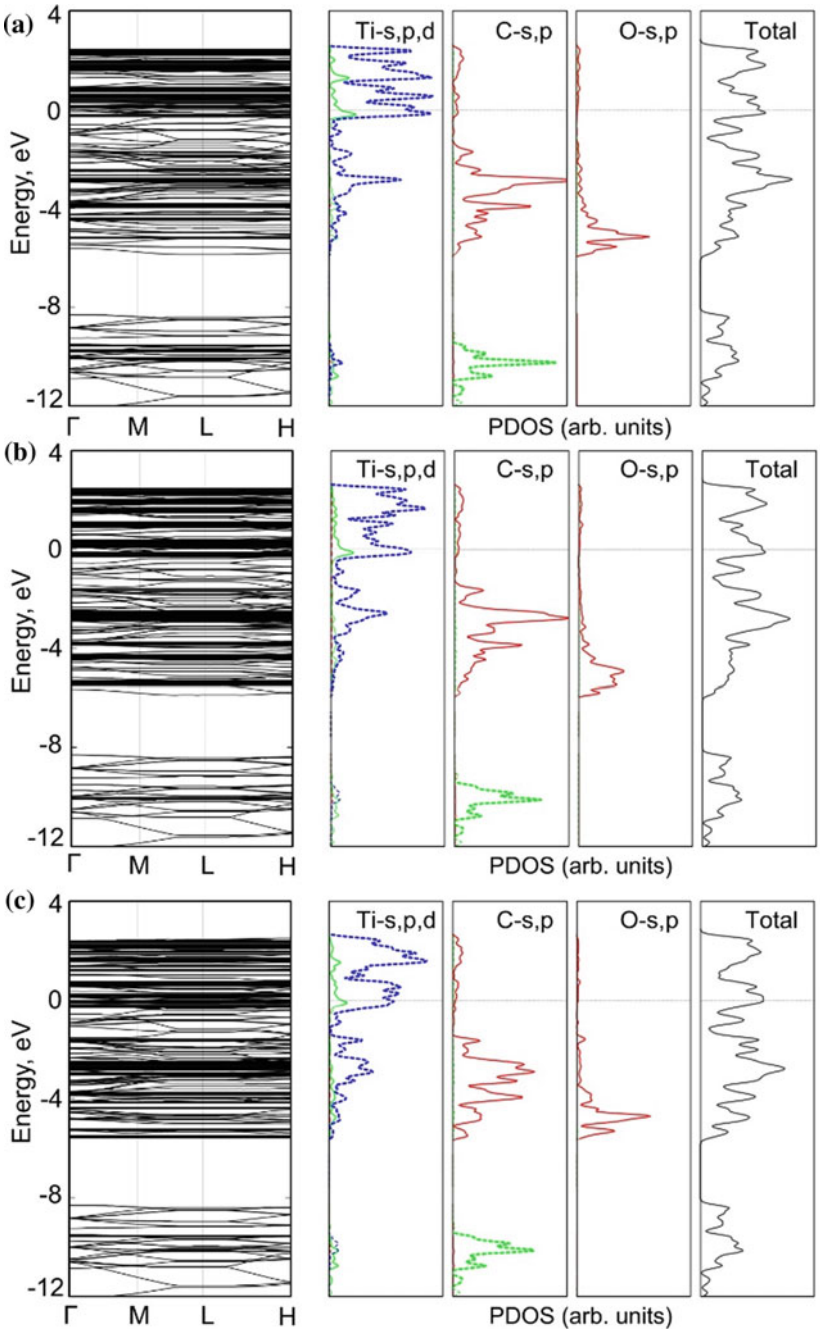

Fig. 11.4 DFT calculations of the band spectrum, partial DOS for Ti, C and O atoms, and total DOS on (111) surface: **a** 3-O/TiC (triangle, FCC site), **b** 3-O/TiC (trimer, FCC site), **c** 3-O/TiC (triangle, HCP site); partial DOS: s—green, p—red, d—blue, total DOS—black

oxygen atom and its nine nearest neighbors is d_{O-Ti} = 2.02 Å. Energies of the hybridized ground state of C_{2p}–Ti_{3d} electrons in this atomic structure configuration and in the configuration in Fig. 11.2g appear to be identical. However, in this configuration (Fig. 11.2i) the Ti–O chemical bond is largely covalent, as indicated by the shape of the electron energy spectrum in Fig. 11.4c. The electron energy spectrum contains three maxima in the −(3.5–5.6) eV interval of energies of the total DOS curve, which in our opinion determine the character and intensity of the chemical bond between the oxygen cluster and TiC(111) film surface.

11.3.3 Elastic Properties of the O/Ti_xC_y(111) Surface

In the present work we have shown that adsorption of atomic O on the non-ideal Ti_xC_y(111) surfaces in different binding positions results in considerable change of the local atomic structure and the band structure as well as total energy of the O/Ti_xC_y(111) systems. Analysis of Tables 11.1 and 11.2 additionally shows that the bond length d_{Ti-C} in 2D lattice of Ti_xC_y(111) demonstrates dependence upon the position of oxygen on the surface under study. It can be assumed that by variation of the bond length d_{Ti-C} we can control elastic properties of the O/Ti_xC_y(111) and O/TiC(111) systems. In this section we employed DFT total energy calculations of deformed structures and Elastic software [22] in order to study the elastic properties of reconstructed TiC(111) surfaces. We have calculated elastic moduli: bulk modulus B, Young's modulus E, shear modulus G, and Poisson ratio υ, which are essential properties of mechanical and dynamic characteristics of crystals [2]. First of all, we calculated elastic constants c_{11}, c_{12}, and c_{44}, which were used to calculate elastic moduli. The latter satisfies the conditions of mechanical stability for cubic systems in accordance with [23]:

$$c_{11} > 0, \quad c_{44} > 0, \quad c_{11} - c_{12} > 0, \quad c_{11} + 2c_{12} > 0. \tag{11.2}$$

Elastic constants for the reconstructed TiC surfaces under study are present in Table 11.3. For comparison we also provide elastic constants for an ultrathin 2D TiC(111) slab and a 3D TiC crystal.

The first column of Table 11.3 contains atomic configurations ordered from the top down depending on the length d_{Ti-C} of the Ti–C bond provided in the second column. For calculation of elastic constants, we used the parameters of a simulated unit cell (column 3) equal to doubled length d_{Ti-C} of the Ti–C bond in the atomic configurations under consideration. For the bond length d_{Ti-C}, we used its value between three top Ti and C layers. In order to find the average bond length d_{Ti-C}, we used 40 pairs of Ti and C atoms. Calculated elastic constants c_{11}, c_{12}, and c_{44} characterize the entire reconstructed top layer (comprising three monolayers, i.e. two Ti monolayers and one C monolayer) of ultrathin TiC(111) band with atomic oxygen coverage of 0.11 ML. These elastic constants were used to calculate the

Table 11.3 Average bond length, d_{Ti-C} (Å); lattice parameter a (Å); elastic constants c_{11}, c_{12}, c_{44} (GPa); elastic moduli B, G, E (GPa); Poisson's ratio υ for the top layer in various atomic configurations of the O/Ti_xC_y(111), O/TiC(111), 2D TiC(111), 2D TiC(001) systems, and in a TiC crystal

Site	d_{Ti-C} (Å)	a (Å)	C_{11}	C_{12}	$C_{11}-C_{12}$	C_{44}	B	G	E	υ
			GPa							
O/TiC(A)	2.150	4.300	593.7	122.3	471.4	193.5	279.4	209.4	502.6	0.20
O/TiC(B)	2.153	4.306	564.4	120.4	444.0	187.9	268.4	200.8	482.3	0.20
O/TiC(C)	2.152	4.304	567.9	120.6	447.3	188.5	267.7	201.9	484.7	0.20
O/TiC(D)	2.152	4.304	567.9	120.6	447.3	188.5	267.7	201.9	484.7	0.20
O/Ti_xC(A, Ti_{vak})	2.142	4.284	605.5	122.6	472.9	195.5	283.5	212.8	510.56	0.20
O/TiC_x(C, C_{vak})	2.150	4.300	575.6	120.9	454.7	189.9	272.5	204.1	489.9	0.20
2D TiC(111)	2.139	4.278	615.8	123.4	482.4	197.5	287.5	215.8	520.2	0.20
2D TiC(001) [15]	2.155	4.310	557.4	119.8	437.7	186.5	265.65	198.82	477.38	0.20
3D TiC(theory)	2.165	4.330	522.2	117.8	404.4	179.9	252.56, 251.4 [3]	188.51, 205.7 [3]	452.65, 481.4 [3]	0.20, 0.181 [3]
3D TiC(test)	2.165	4.33 [23]	500 [25]	113 [25]	387 [25]	178.3 [25]	242.0 [25]	182 [25]	437 [26]	0.199 [26]

bulk modulus B, Young's modulus E, shear modulus G, and Poisson's ratio υ, summarized in Table 11.3.

Analysis of the data in Table 11.3 allows one to note some peculiarities. In particular, elastic constants c_{11}, c_{12}, c_{44}, bulk modulus B, Young's modulus E, shear modulus G, decrease with the increase of the bond length $d_{\mathrm{Ti-C}}$ between Ti and C atoms. Dependence of elastic constants and elastic moduli upon the length $d_{\mathrm{Ti-C}}$ of the bond between Ti and C atoms is illustrated in Fig. 11.5. The largest change is exhibited by the elastic constant c_{11} and Young's modulus E, the smallest change is typical of the c_{12} elastic constant (see Fig. 11.5a). Poisson's ratio υ does not change for these atomic configurations, remaining at $\upsilon = 0.20$ and matching the υ coefficient value for ultrathin 2D TiC(111) band and a 3D TiC crystal.

In our opinion, the elastic constants and elastic moduli in Table 11.3 can characterize elastic properties of the surface, affected by laser radiation. It is appropriate to summarize the potential physical mechanisms of nanostructuring, based on the previous results. Let us consider the pristine 3D TiC crystal, characterized by the lattice parameter $a = 4.330$ Å, which corresponds to the Ti–C bond length $d_{\mathrm{Ti-C}} = 2.165$ Å. This bond length is characteristic of the equilibrium crystal structure of 3D TiC, which we accept as the reference for the $d_{\mathrm{Ti-C}}$ bond length values. Left part contains atomic configurations, corresponding to smaller bond lengths and higher values of the elastic moduli (see Fig. 11.5b). Total energy of Ti-terminated stoichiometric 2D TiC(111) is −3456.5663 Ry after relaxation.

The state corresponds to the smallest bond length $d_{\mathrm{Ti-C}} = 2.139$ Å and to maximum values of elastic moduli (see Table 11.3). The results of our similar calculation for TiC (001) surface are also provided here. A comparison was performed between the values of elastic moduli B, G, and E for (111) and (001) stoichiometric 2D TiC surfaces. Analysis has shown that elastic moduli B, G, and E of Ti-terminated (111) surface exceed the corresponding moduli for (001) surface by 21.85, 16.98, and 42.82 GPa, respectively.

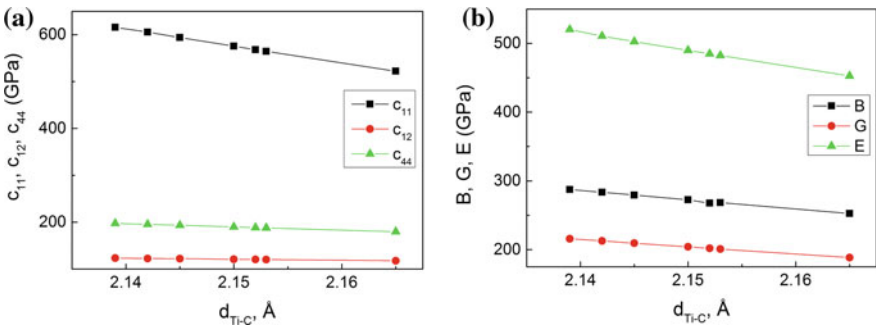

Fig. 11.5 Dependence of elastic constants (**a**) and elastic moduli (**b**) upon the length of the Ti–C bond in atomic configurations of O/Ti_xC_y(111), O/TiC(111), TiC(111) systems, and in a TiC crystal

The processes of titanium carbide nanostructuring with laser in the air may involve different mechanisms of surface reconstruction forming new material properties. Submicrometer structures are known [27] to appear on the surface in two cases—in the mode below the ablation threshold when melt is present in the affected area, and in the ablation mode, characterized by removal of surface fragments. This paper is devoted to the first case, which is typically characterized by the presence of a molten pool. According to the theoretical findings of [28], carbon atoms evaporate several times faster than titanium atoms. Therefore, carbon atoms will be ejected from the molten pool more often than titanium atoms. In our view, crystallization of TiC(111) surface may result in vacancies, which can appear both in the carbon and the titanium sublattices. The number of carbon vacancies at that must be higher than the number of titanium vacancies. In this connection, the following mechanism of surface reconstruction appears to be most probable (*first mechanism*): carbon atoms may be "ejected" from the surface melt layer creating a vacancy in the second layer from the (111) surface top. An oxygen atom may take up a position above such vacancy (see Fig. 11.2e). As DFT calculation has demonstrated, the process is accompanied with a decrease of the Ti–C bond length to $d_{\mathrm{Ti-C}}$ = 2.150 Å for surface atoms. According to Fig. 11.5b, this bond length value corresponds to higher values of elastic moduli relatively to a titanium carbide crystal. The increase in the values of elastic moduli for the O/TiC_y(001) configuration reaches 8% compared with a 3D TiC crystal. The effect can be viewed as a nanostructuring process. In that case total energy of the calculated cell in the O/TiC_y(001) system decreases to −3477.3891 Ry, indicating preference of this process in terms of energy. It should also be noted that the adsorption energy for atomic oxygen in this configuration has maximum value (−11.06 eV/atom) among the examined reconstructions. In particular, the chemical bond energy of the oxygen atom in the O/TiC_y(001) atomic configuration is E_{coh} = 5.7 eV, indicating the presence of a tight chemical bond.

Second mechanism: during laser evaporation of a surface titanium atom one can observe a reconstruction of the local O/Ti_xC(111) atomic structure, where the oxygen atom occupies the position above the titanium vacancy of the first layer (see Fig. 11.2b). In that configuration the averaged length of the Ti–C bond reached $d_{\mathrm{Ti-C}}$ = 2.142 Å for surface atoms. The increase in the values of elastic moduli for the O/Ti_xC(111) configuration is over 12% relatively to a 3D TiC crystal. The effect can also be viewed as a nanostructuring process. In this case, total energy of the calculated cell for a O/Ti_xC(111) system increases to −3371.6716 Ry, as determined by nonstoichiometry following from the loss of the titanium atom during laser evaporation. In this configuration the adsorption energy of atomic oxygen turned out to be minimal (−5.14 eV/atom) in the O/TiC(111) system. In particular, the chemical bond energy of the oxygen atom in the O/Ti_xC(111) atomic configuration is E_{coh} = 2.3 eV, indicating the presence of a chemical bond.

Third mechanism: an oxygen atom has accidentally appeared in a position above carbon atom (HCP hollow) in the second (111) surface layer. The bond length $d_{\mathrm{Ti-O}}$ is 2.01 Å. That atomic configuration (Fig. 11.2d) is characterized by an averaged length of the Ti–C bond of $d_{\mathrm{Ti-C}}$ = 2.09 Å for surface atoms. The increase in the

values of elastic moduli for the O/TiC(111) configuration is over 6%, which can be considered as a nanostructuring effect. Total energy of the O/TiC(111) system is −3488.8641 Ry. The oxygen atom adsorption energy in this configuration is E_{ads} = −9.85 eV/atom.

Fourth mechanism: an oxygen atom, which has accidentally appeared in a bridge binding site (see Fig. 11.2f), forms a sufficiently stable atomic configuration. The length of the bridge forming bond is d_{O-Ti} = 1.97 Å. The energy of the oxygen atom adsorption on TiC(001) surface in the bridge binding site is E_{ads} = −10.68 eV/atom. That configuration is characterized by an averaged length of the Ti–C bond of d_{Ti-C} = 2.06 Å for surface atoms. The increase in the values of elastic moduli for the O/TiC(111) configuration reaches 6%. Total energy of the O/TiC(111) system is −3488.9249 Ry.

Fifth mechanism: an oxygen atom, which has appeared in a position above a titanium atom, forms a TiO_x oxide with the bond length d_{Ti-O} = 1.71 Å. At such distance chemisorption processes can occur and result in creation of a TiO_x compound, as confirmed in [28]. That configuration is characterized by an averaged length of the Ti–C bond d_{Ti-C} = 2.15 Å for surface atoms, and an increase in the values of elastic moduli by over 10%. Total energy of the O/TiC(111) system in this configuration is −3488.7557 Ry.

11.4 Conclusion

In the present work the ab initio calculations based on the density functional theory were performed and the Lagrangian elasticity theory (within the framework of ElaStic) was applied in order to study the local atomic structure, thermodynamic, electronic, and elastic properties of non-stoichiometric O/Ti_xC_y(111) systems in different surface reconstructions. Nine possible reconstructions of TiC surface were considered. The reconstructions were simulated by placement of atomic oxygen on the surface, simulating potential laser reconstructions of the surface.

It has been demonstrated that adsorption of atomic oxygen upon nonideal Ti_xC_y(001) surfaces in different binding positions results in considerable reordering of the local atomic structure and the band spectrum. The rearrangement determines the total energy of generated configurations. For the first time a correlation between the energy level of flat bands in the −5.1 and −5.7 eV energy regions was established, responsible for the double singular peaks of partial densities of oxygen 2*p* electrons, and the bond energy E_{coh} of O atom in non-stoichiometric O/TiC_y(111) systems. In this configuration, the main part of partial DOS of C and Ti atoms is in the −1.9 to −3.7 eV interval of energies. This feature determines the basic properties of the O/TiC_y(111) system. The −4.5 to −5.7 eV interval of energies shows mixing between partial states of O, C, and Ti electrons, which plays a decisive role in forming of the corresponding chemical bond and adsorption energy. The revealed correlation plays an important role in the understanding of the chemical bond character and oxygen atom adsorption onto a non-stoichiometric

TiC(111) surface. DFT-based calculations established a considerable rearrangement in the local atomic structure of O/TiC(111) surface depending upon the degree of its coverage with atomic oxygen. We have demonstrated that the distance between adsorbate and TiC(111) surface decreases with the increase of coverage with oxygen. In our view, atomic structure reconstruction may be caused by charge transfer from Ti atoms to C atoms, resulting in stronger electrostatic interaction between Ti and C atoms.

In the present work, the effective charges of Ti and C atoms surrounding the oxygen adatom in different reconstructions have been identified. Based on DFT calculations, the charge transfer from Ti to O and C atoms have been established, which is caused, in our opinion, by the reconstruction of atomic and electronic structures; it correlates with the electronegativity of the studied atoms. Investigation of the chemisorption processes is of the greatest interest in case of non-stoichiometric $TiC_y(001)$ with the oxygen atom located above the carbon atom vacancy in the second layer. Relaxation results in oxygen atom substitution in the bridge site to formation of the bond length $d_{O-Ti} = 1.94$ Å. The oxygen atom in that position accumulates a considerable effective charge of −0.79e. The nearest titanium and carbon atoms accumulate effective charges of +0.92 and −1.12e, respectively. This configuration corresponds to the largest adsorption energy value of $E_{ads} = -11.06$ eV/atom, which in our opinion is determined by the change in the local atomic structure.

The bond lengths have been established for 40 pairs of Ti and C atoms of three upper layers in six examined O/TiC(111) configurations. We have checked the hypothesis suggesting a relation between elastic moduli and the length of the bond between titanium and carbon atoms, as well as its applicability in order to evaluate elastic properties of a reconstructed top layer of $O/Ti_xC_y(111)$ surface depending upon the position of atomic oxygen thereon. Potential mechanisms for laser nanostructuring of titanium carbide surface have been suggested.

References

1. X. Yuan, L. Cheng, L. Zhang, J. Alloy Compd. **622**, 282 (2015)
2. J. Xiao, B. Jiang, K. Huang, H. Zhu, Comput. Mater. Sci. **88**, 86 (2014)
3. J. Kim, S. Kang, J. Alloy Compd. **528**, 20 (2012)
4. L.S. Marques, A. Fernandes, F. Vaz, M. Ramos, Plasma Processes Polym. **4**, S195 (2007)
5. L. Wang, L.-H. Fang, J.-H. Gong, Trans. Nonferrous Metals Soc. China **22**, 170 (2012)
6. H. Ye, G. Chen, Y. Zhu, S.-H. Wei, Phys. Rev. B **77**, 033302 (2008)
7. C.I. Mikoluzhkii, V.Y. Homich, V.A. Shmakov, V.Y. Yamshikov, Russia Nanotechnol. **11/12**, 65 (2011) (in Russian)
8. V.V. Ilyasov, D.K. Pham, Vestnik of DSTU **14**, 72 (2014). (In Russian)
9. S. Zaima, Y. Shibata, H. Adachi, C. Oshima, S. Otani, M. Aono, Y. Ishizawa, Surf. Sci. **157**, 380 (1985)
10. K.E. Tan, M.W. Finnis, A.P. Horsfield, A.P. Sutton, Surf. Sci. **348**, 49 (1996)
11. C. Ruberto, B.I. Lundqvist, Phys. Rev. B **75**, 235438 (2007)
12. R. Souda, C. Oshima, S. Otani, Y. Ishizawa, M. Aono, Surf. Sci. **199**, 154 (1988)

13. K. Edamoto, A. Mochida, T. Anazawa, T. Itakura, E. Miyazaki, H. Kato, S. Otani, Phys. Rev. B **46**, 7127 (1992)
14. J. Ahn, H. Kawanowa, R. Souda, Surf. Sci. **429**, 338 (1999)
15. V.V. Ilyasov, K.D. Pham, O.M. Holodova, I.V. Ershov, Appl. Surf. Sci. **351**, 433 (2015)
16. P. Giannozzi, S. Baroni, N. Bonini, M. Calandra, R. Car, C. Cavazzoni, D. Ceresoli, G.L. Chiarotti, M. Cococcioni, I. Dabo, J. Phys. Condens. Matter **21**, 395502 (2009)
17. J.P. Perdew, K. Burke, M. Ernzerhof, Phys. Rev. Lett. **77**, 3865 (1996)
18. J.P. Perdew, A. Ruzsinszky, G.I. Csonka, O.A. Vydrov, G.E. Scuseria, L.A. Constantin, X. Zhou, K. Burke, Phys. Rev. Lett. **100**, 136406 (2008)
19. V.V. Ilyasov, D.K. Pham, O.M. Kholodova, Order. Miner. Alloys **1**, 131 (2014)
20. N. Troullier, J.L. Martins, Phys. Rev. B **43**, 1993 (1991)
21. P.-O. Löwdin, *Advances in Quantum Chemistry*, ed. by L. Per-Olov (Academic Press, London, 1970), p. 185
22. R. Golesorkhtabar, P. Pavone, J. Spitaler, P. Puschnig, C. Draxl, ElaStic. Comput. Phys. Commun. **184**, 1861 (2013)
23. Y. Li, Y. Gao, B. Xiao, T. Min, Z. Fan, S. Ma, L. Xu, J. Alloy Compd. **502**, 28 (2010)
24. Y. Liu, Y. Jiang, R. Zhou, J. Feng, J. Alloy Compd. **582**, 500 (2014)
25. J. Holliday, *Advances in X-Ray Analysiss*, vol. 13. (Plenum Press, New York, 1970), p. 136
26. E. Francisco, M. Blanco, G. Sanjurjo, Phys. Rev. B **63**, 094107 (2001)
27. I.N. Zavestovskaya, Quantum Electron. **40**, 942 (2010)
28. J.A. Rodriguez, P. Liu, J. Dvorak, T. Jirsak, J. Gomes, Y. Takahashi, K. Nakamura, J. Chem. Phys. **121**, 465 (2004)